Pergamon

Geochimica et Cosmochimica Acta, Vol. 64, No. 17, pp. 2993–3005, 2000

0016-7037/00 $20.00 + .00

PII S0016-7037(00)00402-6

Quartz solubility in H_2O-NaCl and H_2O-CO_2 solutions at deep crust-upper mantle pressures and temperatures: 2–15 kbar and 500–900°C

ROBERT C. NEWTON and CRAIG E. MANNING*
Dept. of Earth and Space Sciences, University of California at Los Angeles, Los Angeles, CA 90095-1567 USA

(*Received October* 6, 1999; *accepted in revised form March* 8, 2000)

ABSTRACT—The solubility of quartz in H_2O-NaCl solutions was measured at 2, 4.35, 10 and 15 kbar and 500–900°C, and at NaCl concentrations up to halite saturation, usually greater than 75 wt.%. Quartz solubility was also measured in CO_2-H_2O solutions at 10 kbar and 800°C. Solubilities were determined by weight loss of ground and polished quartz crystal fragments which were equilibrated with solutions in Pt envelopes for one to four days and then rapidly quenched. Experiments at 2 kbar were made with externally heated cold-seal apparatus; higher pressure experiments were done in a ¾ inch-diameter piston-cylinder apparatus with NaCl pressure medium and graphite heater sleeve. Equilibrium solubility was demonstrated in several ways, and the present results reproduce those of Manning (1994) in pure H_2O at selected conditions.

At pressures below 4 kbar, NaCl in solution causes an initial "salting-in", or quartz solubility enhancement, which, at 2 kbar and 700°C, persists to concentrations as great as 70 wt.% NaCl before quartz solubility again becomes as low as in pure H_2O. The maximum solubility occurs at $X(H_2O) \sim 0.9$ and is 50% higher than in pure H_2O. At 4.35 kbar and 700°C, however, quartz solubility decreases slightly with initial NaCl concentration, and then begins to drop rapidly with increasing salinity beyond 45 wt.% NaCl. At 10 and 15 kbar there is a steep initial decline in silica molality at all temperatures in the range 500–900°C, leveling off at higher NaCl concentrations. There is thus a pronounced change in solution behavior with pressure, from initial salting-in below 4 kbar to monotonic salting-out above 5 kbar. This pressure-induced change in silica solubility parallels the sharp decrease in H_2O activity in NaCl solutions in the same pressure range found by Aranovich and Newton (1996). Therefore, the pressure-induced change in silica solubility is inferred to be a consequence of the dissociation of the neutral $NaCl^o$ complex to Na^+ and Cl^- as solution densities increase above about 0.7 gm/cm^3. At very high salinities, approaching halite saturation, the isobars of quartz solubility as a function of NaCl mole fraction at 700°C converge, indicating that, for hypersaline fluids having the constitution of molten salts, pressure has only a minor effect on quartz solubility.

Quartz solubility at 10 kbar shows exponential decline with increasing salinity at all temperatures in the range 500°C to 900°C. This is the expected behavior of a two-component solvent, in which quartz is sparingly soluble in one component. At 10 kbar, isotherms of log silica molality versus H_2O mole fraction are linear between $X(H_2O) = 1.0$ and 0.5, but begin to curve to lower values at 900°C, where high salinities are attained before halite saturation occurs. This behavior implies that the solute silica species is a hydrate that becomes progressively destabilized at low H_2O concentrations of the solvent. Plots of log silica molality versus log H_2O activity suggest that the solute species is neutral H_4SiO_4 with no additional solvated H_2O molecules, assuming no Na-SiO_2 complexing.

The solubility of quartz in CO_2-H_2O fluids at 800°C and 10 kbar is much smaller than in NaCl solutions at the same P,T and H_2O activity. Thermodynamic analysis suggests that the solute species in CO_2-H_2O fluids is H_4SiO_4 with 1–3 solvated H_2O molecules, which is similar to the solute behavior inferred by Walther and Orville (1983) in CO_2 and Ar solutions with H_2O at lower pressures.

The present results show that SiO_2 will partition very strongly into a concentrated salt solution in deep crust-upper mantle metamorphic and metasomatic processes, in preference to a coexisting immiscible CO_2-rich fluid. The much greater permeability of silicate rocks for salt solutions than for CO_2-rich solutions, together with the much higher solubility of silica-rich phases in the former, could be an important factor in geochemical segregation processes involving rising and cooling fluids of magmatic or metamorphic origin.

1. INTRODUCTION

The aqueous solubility of silica is one of the most important parameters in modeling metasomatism and fluid-rock interactions in the outer parts of the earth. Calculations of mass transport in regional metamorphism (Ague, 1994), oceanic hydrothermal systems (Lowell et al., 1993), and subduction complexes (Sorensen, 1988; Manning, 1995; 1997) require knowledge of silica concentration in migrating fluids under a broad range of pressure-temperature conditions.

The major source of information on quartz solubility as a function of pressure and temperature has been experimental studies in pure water, starting with the low-pressure studies of Kennedy (1950) and Morey and Hesselgesser (1951), through the work of Anderson and Burnham (1965) to 9 kbar and 900°C, to that of Manning (1994) to 20 kbar and 900°C. All of these studies used the weight-loss method, in which a ground fragment or crushed aggregate of natural quartz was equilibrated with initially pure water for several hours to a few days

*Author to whom correspondence should be addressed (manning@ess.ucla.edu).

and then swiftly cooled to room temperature in several seconds to tens of minutes, depending on the type of apparatus. The combined dataset of earlier observations was summarized by Manning (1994) in a single equation, in which the solubility of quartz is expressed as an empirical function of temperature and water density.

Natural aqueous fluids are not pure water, but complex mixtures with other volatile species, such as CO_2, and dissolved mineral components, especially alkali and alkaline earth halides and carbonates. Sampling of fluids in geothermal areas (e.g., Fournier, 1987) and modern fluid inclusion studies have shown that NaCl-dominated brines occur in many different petrogenetic settings. The latter technique has revealed that concentrated brines are associated with some sulfide ore bodies (Roedder, 1971), alkaline igneous rocks (Lowenstern, 1994; Belkin et al., 1997), carbonatites (Samson et al., 1995), high-grade metamorphic rocks (Smit and Van Reenen, 1997), peridotites, as at Zabargad Island, Red Sea (Sciuto and Ottonello, 1995), alpine eclogites (Philippot and Selverstone, 1991), and the ultra-high-pressure metasediments of the Western Alps (Philippot et al., 1995). Saline fluid inclusions from these different kinds of rocks typically contain halite and/or sylvite daughter crystals and have bulk compositions with NaCl contents as high as 80 weight percent. These hyperconcentrated brines could equally well be termed "hydrosaline magmas" (Roedder, 1971). Suites of apparently coeval concentrated brines and CO_2-rich fluid inclusions have been reported from some high-grade rocks (Crawford and Hollister, 1986; Touret, 1985).

Experiments on synthetic fluid inclusions in the system H_2O-CO_2-NaCl in quartz crystals indicate that immiscible brine and CO_2-rich fluids can coexist at pressures of 7 kbar and temperatures of at least 900°C (Gibert et al., 1998). The two contrasting types of fluid have greatly differing mechanical properties in relation to silicate rocks. CO_2-rich fluids have low grain-wetting ability (high dihedral angles), whereas concentrated salt solutions have extraordinary infiltration ability (Watson and Brenan, 1987). Partitioning of silica and other major and trace components of rocks between the immiscible fluids is therefore an important consideration for modeling metasomatic processes.

The solution of quartz into a host fluid is described formally by the reaction:

$$SiO_2\,(\text{quartz}) + nH_2O = SiO_2 \cdot nH_2O\,(\text{aqueous}) \qquad (1)$$

The solute species is thought to be dominantly a neutral complex represented by the formulas $Si(OH)_4$ or H_4SiO_4 with one to three hydrogen-bonded (solvated) water molecules. Thus, n in Eqn. (1) may be as high as 5. The hydration state of aqueous silica was investigated by Walther and Orville (1983) from existing quartz solubility data in the system CO_2-H_2O and their own data for Ar-H_2O. Most of the experimental data in CO_2-H_2O solutions are contained in an unpublished M.S. thesis (Shettel, 1974), which presents experimental data to 5 kbar and 900°C. They reveal generally low solubility in CO_2-rich fluids, increasing with T and P at constant $X(H_2O)$. Most of the data plot with slopes of 3 to 4 on isothermal, isobaric diagrams of log silica molality versus log H_2O activity, which Walther and Orville (1983) interpret as indicating that the dominant dissolved molecular silica species has one to two solvated H_2O molecules. This analysis assumes that there is no solute interaction (complexing) between dissolved silica and the diluting volatile, CO_2 or Ar.

Two previous studies are available on the solubility of quartz in concentrated NaCl solutions at supercritical temperatures and pressures. The Novgorodov (1977) measurements at 1.5 kbar and 700°C cover the salinity range 0–13 mole% NaCl. He found that NaCl substantially increases the solubility of quartz at these conditions. This unique "salting in" is most pronounced at low NaCl concentrations. Xie and Walther (1993) present measurements in dilute NaCl solutions (maximum of 0.83 molal or 1.5 mole% NaCl). The maximum temperature and pressure of the study are 2 kbar and 573°C. They found that NaCl initially increases the solubility of SiO_2 over that in pure H_2O at 1 kbar at $>$300°C and decreases it at $<$300°C. This behavior is quite in contrast to that of CO_2 solutions. Anderson and Burnham (1967) found a similar solubility enhancement in KCl solutions at 3 kbar and 600°C. Such salting-in behavior is observed to a more limited extent at 150–350°C at or near H_2O liquid-vapor saturation (e.g., Chen and Marshall, 1982; Fournier et al., 1982; Saccocia and Seyfried, 1990).

Two distinct mechanisms were proposed to explain the silica "salting-in" effect. Anderson and Burnham (1983) invoked a reaction between solute NaCl or KCl and quartz to produce an alkali-silica hydrous complex and hydrochloric acid:

$$SiO_2\,(\text{quartz}) + NaCl + H_2O = H_3NaSiO_4 + HCl \qquad (2)$$

No salting-in effect exists at 25°C and one bar; therefore Anderson and Burnham (1983) concluded that increasing temperature and/or pressure promote salting-in. Xie and Walther (1993) ascribed the salting-in to the action of charged ions on the dielectric constant of the solution, without complex formation other than solvation. Their experiments suggest that solution density, rather than temperature and pressure independently, may be a controlling factor, in that salting-in begins at higher temperature at higher pressure: the change from salting-out to salting-in occurs near 300°C at 0.5 kbar, and above 400°C at one kbar. The cross-over density may therefore be about 0.7 gm/cm^3.

The present study extends the measurements of silica solubility in NaCl solutions to the temperature and pressure regimes of the deeper crust and upper mantle, and to the higher salinity ranges indicated by the fluid inclusion studies on rocks of deeper provenance. Particularly important is the characterization of the effects of temperature, pressure and solution composition on the silica solution enhancement. Another important correlation to be made is with the pronounced pressure-induced decrease of H_2O activity in NaCl and KCl solutions above 3–4 kbar found by Aranovich and Newton (1996, 1997). This activity change could affect the solution properties of SiO_2 by either the mechanism proposed by Anderson and Burnham (1983) or that of Xie and Walther (1993). We have measured quartz solubility in NaCl solutions at conditions of 2–15 kbar and 500–900°C and NaCl concentrations up to halite saturation (at most conditions, greater than 75 wt.% NaCl). We also determined quartz solubility in CO_2-H_2O solutions at 10 kbar and 800°C by the same method to compare quartz-saturated silica contents and solution mechanisms in the contrasting fluids.

2. EXPERIMENTAL METHODS

The methods of the present study follow those of Manning (1994), except for a substantial reduction of the fluid volumes and crystal weights. Experiments from 4 to 15 kbar were made in a ¾ inch diameter piston-cylinder apparatus with NaCl pressure medium and cylindrical graphite heater sleeve. Experiments at 10 and 15 kbar were made under piston-out conditions; that is, assemblies were pressed cold to a pressure 3 kbar less than the desired final pressure. Thermal expansion of the assemblies in heating increased the pressure to the final value. During heating at temperatures above 600°C, some bleeding of pressure was required to maintain the desired value. Under these conditions the pressure apparatus is virtually frictionless; that is, no pressure correction need be applied to the gauge or nominal pressure (Johannes, 1973; Mirwald et al., 1975). In all experiments, it was necessary to consolidate the assemblies at a minimum of 5 kbar before heating so that a large amount of bleeding was required to reduce the pressure to a nominal 4 kbar at the final temperature. The highest sample temperature readily obtainable at 4 kbar was limited to 750°C by the extensional stresses produced in the decompression.

The anomalous pressure-temperature path necessary to achieve a pressure below 5 kbar in the piston-cylinder apparatus makes independent pressure calibration necessary. Calibration was based on the P-T curve for the brucite to periclase dehydration reaction, as accurately determined in a gas-pressure apparatus by Aranovich and Newton (1996). Capsules containing coarsely crystalline periclase made by an arc-fusion process plus excess H_2O exactly emulated the experimental capsules of the present study. Calibration experiments were of the same duration as the solubility measurements: one to two days. If a quenched capsule contained abundant coarse brucite, the stability field of that mineral was considered to have been encountered, inasmuch as the transition is quite rapid with small temperature overstep above 600°C and several kbar. Calibration experiments at a nominal pressure of 4.0 kbar yielded an equilibrium reaction temperature of 727 ± 3°C, corresponding to a pressure of 4.35 ± 0.15 kbar. Maximum pressure uncertainties at all pressures are believed no greater than ±0.3 kbar.

Temperature was measured and controlled by calibrated matched pairs of W-3%Re versus W-25%Re thermocouples. The stated accuracy of the manufacturer (Engelhard) was better than 1°C. A precise digital millivoltmeter in parallel with a Love proportional controller consistently showed a temperature ripple of ±1°C, with a period of 30 sec. The thermocouple was in virtual contact with the quartz crystal: typically, the thermocouple tip made a slight dent in the Pt sample envelope. Maximum uncertainty in sample temperatures from all sources was ±3°C. Quench times were very fast: temperatures fell below 200°C in about 12 sec. after turning off the heating power.

Experiments at 2 kbar were made in externally heated cold-seal bombs. The bombs were mounted horizontally, with the samples at the pre-determined plateau of temperature. Temperatures were measured and controlled by external chromel-P-alumel thermocouples inserted in a well in the bomb at the sample position. Internal metal rods filled the bomb cavity adjacent to the samples. Pressures are accurate to ±50 bars, and temperatures to ±3°C. Quench was by air-blow, and required three minutes to bring the temperature to below 200°C. Pressure was maintained during the quench.

Two large, gemmy natural quartz crystals, one from Brazil (Manning, 1994) and the other from Mountain Valley, AR, provided samples. Small equant chips were ground into ellipsoidal shapes by rolling between sheets of 240-grit emery paper. The crystals were then rolled between sheets of 600-grit paper until they acquired a fair polish. Weights of experimental crystals were mostly 0.3 to 3.5 mg. Larger crystals occasionally broke during the experiments, sometimes during the quench or upon decompression, to judge from unetched conchoidal fractures. A weighed quartz ellipsoid was placed in a 1.3 cm long Pt tube segment of 2 mm diameter and 0.18 mm wall thickness with weighed amounts of multiply-distilled and deionized H_2O, usually about 10 mg, and reagent-grade (Baker ACT) NaCl, previously dried for an hour at 310°C. The capsule was sealed by arc-welding and folded double to produce a packet 2 mm thick and 5 mm square. All weighings were made on a Mettler M3 microbalance, with 1σ reproducibility of 0.002 mg. H_2O contents were determined in two ways, by weighing after loading with a microliter syringe, making a calibrated allowance for loss by evaporation, and by weight loss of punctured quenched capsules dried for 15 min. at 115°C and then for 15 min. at 310°C. The two methods generally yielded the same H_2O contents within 0.5%. The puncture-and-dry weighings were considered to be the more reliable, except for an occasional large discrepancy, which could usually be traced to loss of NaCl from a capsule during drying.

The experiments regarded as definitive were those in which a single unbroken quartz crystal was retrieved from the quenched capsule. Quartz solubility in these experiments was determined from the weight lost by the retrieved crystal. In a few runs, one or a number of small terminated quartz crystals nucleated and grew independently of the seed crystal, probably because of a small temperature gradient across the capsule. Inasmuch as it was usually impossible to be sure that all such small crystals were accounted for, the net weight loss was uncertain. These runs were repeated, as were the few runs in which there was a detectable weight loss of the capsule, signifying a leak.

Experiments at the lowest H_2O percentages were halite-saturated, as shown by the presence of a single large rounded halite crystal, in addition to the quartz crystal, amid the mass of small skeletal salt crystals quenched from the fluid phase. Halite saturation limits the NaCl concentration at a fixed pressure and temperature, but affords the advantage that the fluid compositions at halite saturation are well known, as determined experimentally by Koster Van Groos (1991) and Aranovich and Newton (1996).

A number of experiments were made with quartz crystals sealed with mixtures of liquid water, oxalic acid dihydrate, $2COOH.2H_2O$, and silver oxalate, $Ag_2C_2O_4$, to generate fluids on the join H_2O-CO_2. Under conditions of high oxygen fugacity, oxalic acid dihydrate yields a fluid of equimolar CO_2 and H_2O, with outward diffusion of hydrogen through the Pt capsule walls. Silver oxalate yields pure CO_2 and silver metal. Fluid ingredients plus a quartz crystal were sealed without significant weight loss in short segments of 1-mm-diameter Pt tubing. Because of space limitations, crystal weights were only 0.3–0.5 mg. Typical volatile contents were 3–5 mg. The Pt capsules were in turn loaded into segments of 3 mm diameter Au tube with about 40 mg of hematite and 4 mg of H_2O, and sealed by welding. The resulting buffer capsules had geometries nearly identical to the larger Pt capsules of the unbuffered runs. At the conclusion of the runs, the quenched buffer capsules were checked for leakage, and to verify that hematite and magnetite were both present, constituting an HM buffer. Retrieved Pt capsules were inflated with CO_2 pressure, unless there was leakage during or after the run. Fluids were analyzed by the puncture-weight loss technique described by Aranovich and Newton (1999). First, a capsule was frozen in liquid nitrogen and punctured with a needle while still frozen. During warming, an immediate weight loss was ascribed to CO_2 escape. The capsules were dried at 115°C and then at 310°C for 15 min. each and reweighed to obtain the H_2O content. The H_2O content determined in this way agreed with the initially loaded value to within ±0.12 mg.

3. RESULTS OF SOLUBILITY MEASUREMENTS

3.1. Weighing Uncertainties, Reproducibility, and Equilibration

Tables 1 and 2 list data for the experiments with NaCl- and CO_2-bearing aqueous solutions, respectively, including molality values calculated from (crystal weight loss)*1000/(60.085*(weight H_2O)). Fluid inclusions trapped during experiments were too few and tiny to influence solubility determinations. Uncertainties due to weighing were estimated numerically. Replicate weighings of solids yielded a normal distribution of weighing errors with $1\sigma = 0.002$ mg. The difference between the initial H_2O weight, determined by applying an evaporation correction, and the weight determined after each experiment by drying was also normally distributed and averaged −0.065 mg with $1\sigma = 0.079$ mg. This discrepancy suggests that we overcorrected for evaporation loss, either because addition of NaCl after water decreased the rate of evaporation from the capsule or, despite drying, a small amount

Table 1. Quartz solubility measurements in H_2O-NaCl fluids.

Expt. no.	P (kbar)	T (°C)	Time (hr)	Initial qz wt. (mg)	Final qz wt. (mg)	Initial H_2O wt. (mg)	Initial NaCl wt. (mg)	X_{H_2O}	a_{H_2O}	X_{NaCl}	$10^3 * X_{SiO_2}$	m_{SiO_2} (mol/kgH_2O)
45	2	700	91	0.306	0.247	7.057	0.000	0.997	0.997	0.000	2.5 (3)	0.139 (15)
56	2	700	96	1.713	1.567	11.301	2.449	0.934 (1)	0.944 (1)	0.062 (1)	3.6 (2)	0.215 (10)
48	2	700	96	2.150	2.057	7.403	4.497	0.840 (4)	0.862 (4)	0.157 (4)	3.2 (2)	0.209 (15)
47	2	700	96	0.483	0.402	9.307	17.589	0.631 (6)	0.671 (6)	0.368 (6)	1.6 (1)	0.145 (11)
49	2	700	96	2.792	2.759	7.036	24.377	0.483 (8)	0.527 (8)	0.516 (8)	0.7 (1)	0.078 (15)
61	4.35	600	46	0.873	0.725	11.276	0.000	0.996	0.996	0.000	3.9 (2)	0.219 (10)
59	4.35	600	43	2.019	1.929	11.108	14.531	0.711 (4)	0.594 (4)	0.287 (4)	1.7 (1)	0.135 (9)
56	4.35	600	47	1.783	1.722	10.741	20.332	0.631 (5)	0.504 (5)	0.368 (5)	1.1 (1)	0.095 (9)
43	4.35	700	19	0.927	0.714	9.421	0.000	0.993	0.993	0.000	6.7 (3)	0.377 (14)
60	4.35	700	21	1.719	1.477	11.066	3.345	0.909 (2)	0.884 (2)	0.085 (2)	6.0 (2)	0.364 (12)
46	4.35	700	23	1.851	1.710	6.993	4.424	0.833 (4)	0.789 (4)	0.162 (4)	5.0 (3)	0.336 (18)
70	4.35	700	23	1.608	1.431	10.836	11.721	0.747 (4)	0.688 (4)	0.249 (4)	3.7 (1)	0.272 (11)
41	4.35	700	18	1.932	1.849	6.809	11.295	0.660 (7)	0.591 (7)	0.338 (7)	2.4 (2)	0.203 (16)
42	4.35	700	72	0.268	0.233	4.932	16.185	0.497 (11)	0.424 ((11)	0.502 (11)	1.1 (2)	0.118 (21)
72	4.35	750	15	2.175	1.728	16.266	0.000	0.992	0.992	0.000	8.2 (2)	0.458 (9)
69	4.35	750	22	1.929	1.526	18.245	18.000	0.763 (2)	0.726 (2)	0.232 (2)	5.1 (1)	0.368 (7)
77	4.35	750	25	1.237	1.189	7.169	34.158	0.405 (7)	0.358 (7)	0.594 (8)	0.8 (1)	0.112 (15)
M94	10	500	25	19.945	19.291	63.688	0.000	0.997	0.997	0.000	3.1	0.171 (2)
M94	10	500	262	9.452	8.684	73.952	0.000	0.997	0.997	0.000	3.1	0.173 (2)
68	10	500	70	0.726	0.620	14.795	6.061	0.886 (2)	0.759 (2)	0.112 (1)	1.9 (1)	0.119 (7)
63	*10*	*500*	*93*	*0.763*	*0.713*	*10.783*	*16.174*	*0.78 (2)*	*0.59 (2)*	*0.22 (2)*	*1.1 (1)*	*0.077 (9)*
67	10	600	72	1.083	0.727	16.817	0.000	0.994	0.994	0.000	6.3 (1)	0.353 (8)
37	10	600	69	1.013	0.880	10.995	6.948	0.834 (3)	0.688 (3)	0.163 (3)	3.0 (1)	0.201 (10)
40	*10*	*600*	*48*	*0.293*	*0.209*	*11.148*	*19.372*	*0.67 (2)*	*0.47 (2)*	*0.33 (2)*	*1.5 (1)*	*0.125 (9)*
52	10	700	24	2.068	1.608	11.201	0.000	0.988	0.988	0.000	12.2 (3)	0.684 (17)
62	10	700	22	1.154	0.797	10.992	2.825	0.918 (1)	0.850 (1)	0.073 (1)	8.9 (2)	0.541 (15)
31	10	700	44	1.037	0.777	10.776	6.695	0.834 (3)	0.710 (3)	0.160 (3)	6.0 (2)	0.402 (13)
30	10	700	24	1.323	1.154	10.513	15.067	0.691 (5)	0.518 (5)	0.305 (4)	3.3 (1)	0.268 (11)
32	*10*	*700*	*72*	*0.618*	*0.559*	*6.238*	*24.384*	*0.56 (2)*	*0.38 (2)*	*0.44 (2)*	*1.6 (2)*	*0.158 (17)*
20	10	800	23	2.108	0.446	22.176	0.000	0.978	0.978	0.000	22.0 (2)	1.248 (13)
26	10	800	20	1.971	1.310	11.084	2.408	0.922 (1)	0.874 (1)	0.062 (1)	16.5 (3)	0.993 (22)
14	10	800	28	2.035	0.830	22.099	8.451	0.882 (1)	0.808 (1)	0.104 (1)	14.4 (1)	0.908 (10)
25	10	800	24	0.800	0.292	10.409	5.705	0.845 (3)	0.751 (3)	0.143 (3)	12.4 (3)	0.813 (20)
9	10	800	26	2.849	2.424	10.848	8.900	0.791 (3)	0.673 (3)	0.200 (3)	9.3 (2)	0.652 (17)
19	10	800	24	1.274	0.907	10.787	11.698	0.744 (4)	0.610 (4)	0.249 (4)	7.6 (2)	0.567 (15)
11	10	800	72	3.618	3.298	11.095	14.910	0.703 (4)	0.560 (4)	0.291 (4)	6.1 (1)	0.480 (14)
16	10	800	23	0.593	0.260	11.149	15.732	0.693 (4)	0.548 (4)	0.301 (4)	6.2 (1)	0.497 (14)
27	10	800	20	1.374	1.082	10.164	14.542	0.690 (5)	0.544 (5)	0.304 (4)	5.9 (2)	0.478 (15)
18	10	800	46	2.746	2.470	11.212	19.962	0.643 (5)	0.491 (5)	0.353 (4)	4.7 (1)	0.410 (12)
24	10	800	27	1.442	1.232	10.502	24.281	0.582 (5)	0.427 (5)	0.415 (5)	3.5 (1)	0.333 (13)
22	10	800	22	0.961	0.763	10.867	29.108	0.546 (5)	0.391 (5)	0.451 (5)	3.0 (1)	0.303 (11)
17	10	800	25	2.523	2.336	11.149	34.734	0.509 (5)	0.356 (5)	0.489 (5)	2.6 (1)	0.279 (11)
21	10	800	53	0.710	0.546	11.272	41.579	0.467 (5)	0.318 (5)	0.531 (5)	2.0 (1)	0.242 (10)
15	*10*	*800*	*46*	*1.024*	*0.888*	*11.200*	*54.282*	*0.42 (2)*	*0.28 (2)*	*0.58 (2)*	*1.5 (1)*	*0.202 (10)*
53	10	850	22	2.614	1.675	9.278	0.000	0.971 (1)	0.971 (1)	0.000	29.5 (7)	1.685 (41)
35	10	850	22	1.340	0.634	11.123	6.594	0.832 (3)	0.744 (3)	0.152 (2)	15.8 (3)	1.057 (23)
34	10	850	22	1.107	0.688	10.775	15.432	0.688 (4)	0.557 (4)	0.304 (4)	8.0 (2)	0.648 (17)
39	10	850	18	1.525	1.281	10.582	30.293	0.529 (5)	0.389 (5)	0.467 (5)	3.7 (1)	0.384 (13)
75	10	850	22	1.323	1.238	5.991	29.551	0.396 (9)	0.270 (9)	0.602 (9)	1.7 (1)	0.236 (19)
36	10	850	21	0.542	0.483	4.763	29.170	0.346 (11)	0.230 (11)	0.653 (11)	1.3 (1)	0.206 (23)
74	*10*	*875*	*20*	*1.727*	*1.674*	*4.773*	*48.170*	*0.30 (2)*	*0.19 (2)*	*0.70 (2)*	*1.1 (1)*	*0.185 (23)*
M94	10	900	17	13.85	7.92	41.25	0.000	0.959	0.959	0.000	41.3 (2)	2.39 (1)
55	10	900	11	3.121	2.493	11.193	12.952	0.728 (4)	0.620 (4)	0.260 (4)	12.3 (2)	0.934 (21)
54	10	900	10	2.360	2.172	7.513	26.699	0.476 (7)	0.352 (7)	0.521 (7)	3.6 (1)	0.417 (19)
76	10	900	20	1.675	1.586	5.902	35.827	0.348 (8)	0.242 (8)	0.651 (8)	1.6 (1)	0.251 (19)
64	*10*	*900*	*14*	*3.039*	*3.012*	*2.947*	*44.556*	*0.24 (2)*	*0.16 (2)*	*0.76 (2)*	*0.7 (2)*	*0.153 (36)*
65	*10*	*900*	*20*	*3.014*	*2.990*	*2.863*	*39.845*	*0.24 (2)*	*0.16 (2)*	*0.76 (2)*	*0.6 (2)*	*0.140 (38)*
M94	15	700	45	20.99	19.21	35.16	0.000	0.985	0.985	0.000	15.0 (1)	0.843 (6)
79	15	700	20	1.190	0.807	10.946	3.435	0.903 (2)	0.797 (2)	0.087 (2)	9.5 (2)	0.583 (15)
50	15	700	22	1.248	0.982	9.496	5.490	0.843 (3)	0.685 (3)	0.150 (3)	7.1 (2)	0.466 (16)
78	15	700	20	1.588	1.406	10.271	13.784	0.705 (5)	0.488 (5)	0.292 (4)	3.7 (1)	0.295 (12)
51	15	700	25	1.576	1.482	6.724	12.595	0.632 (8)	0.406 (8)	0.365 (8)	2.7 (2)	0.233 (17)

Underlined entries from Manning (1994). Italics denote halite saturation. In halite-undersaturated experiments, $X_i = n_i/(n_{H_2O} + n_{NaCl} + n_{SiO2})$, whereas at halite saturation X_{H_2O} and X_{NaCl} were taken from Aranovich and Newton (1996) and ignore SiO_2 in the fluid. a_{H_2O} from Aranovich and Newton (1996) assuming that SiO_2 is an inert diluent. Parenthetical numbers are numerically propagated 2σ weighing uncertainties in last digit(s) where >0.5 (see text) for all values except those at halite saturation, which also include an assumed 2σ uncertainty in X_{H_2O} of 0.2.

Table 2. Quartz solubility measurements in H_2O-CO_2 fluids.

Expt. no.	P (kbar)	T (°C)	Time (hr)	Initial qz wt. (mg)	Final qz wt. (mg)	Final H_2O wt. (mg)	Final CO_2 wt. (mg)	X_{H_2O}	a_{H_2O}	X_{CO_2}	$10^3*X_{SiO_2}$	m_{SiO_2} (mol/kgH_2O)
C-5	10	800	46	0.401	0.316	2.382	1.335	0.806 (1)	0.863 (1)	0.185 (1)	8.6 (6)	0.594 (40)
C-4	10	800	46	0.456	0.413	2.108	2.631	0.659 (1)	0.771 (1)	0.337 (1)	4.0 (5)	0.340 (44)
C-1	10	800	23	0.414	0.391	1.835	4.482	0.499 (1)	0.658 (1)	0.499 (1)	1.9 (6)	0.209 (52)
C-6	10	800	45	0.295	0.278	1.740	4.322	0.495 (1)	0.656 (1)	0.503 (1)	1.5 (5)	0.163 (55)
C-3	10	800	30	0.393	0.389	0.595	3.033	0.324 (2)	0.492 (1)	0.676 (2)	0.7 (9)	0.112 (156)

$X_i = n_i/(n_{H_2O} + n_{CO_2} + n_{SiO_2})$. a_{H_2O} from Aranovich and Newton (1999) assuming that SiO_2 is an inert diluent. Parenthetical numbers are numerically propagated 2σ weighing uncertainties in last digit(s) (see text).

of H_2O was retained in the amorphous silica quench-precipitate. All weighing-related errors were propagated to final concentrations by using a Monte Carlo routine in which 1000 trial weights were generated randomly using population characteristics determined from the weighing checks. Increasing the number of trial weights did not change the results. Final errors are reported in Tables 1 and 2 as 2σ uncertainties that include weighing and evaporative loss of H_2O during capsule loading. The uncertainty given in this study are less than that of Manning (1994), in which $2\sigma = 0.040$ molal, because errors in that study were determined by pooling results of replicate experiments and therefore included uncertainties in pressure and temperature as well.

Two kinds of experiments were made which reproduced the Manning (1994) SiO_2 molality value at 10 kbar and 800°C in pure H_2O. A single weight loss measurement (#20, Table 1) gave $m(SiO_2) = 1.247 \pm 0.013$, compared to the Manning (1994) value of 1.232 ± 0.040 molal, demonstrating excellent agreement. The second kind of experiment introduced finely ground quartz into NaCl-H_2O mixtures in progressively greater amounts in successive runs, with microscopic search for quartz crystals in the quenched charges. The onset of quartz saturation was signaled by the sudden appearance of a few large terminated quartz crystals. This method, though not as precise as the weight loss method, confirmed the validity of the latter method by yielding a molality of 1.23 ± 0.11 in pure H_2O at 800°C and 10 kbar.

Equilibrium solubility was indicated in two ways. A time study was made at $X(H_2O)$ approximately 0.7 (runs 11, 16 and 27, Table 1). The initial weights of the quartz crystals ranged from 3.6 to 0.6 mg. Times ranged from 20 to 72 h. The results were identical within analytical errors. A more comprehensive proof of the attainment of equilibrium solubility was the appearance, in the majority of experiments, of broad, shiny crystal faces usually on one or both ends of the ellipsoidal quartz crystal, despite overall weight loss. This evidence of solution and reprecipitation is virtual proof of quartz saturation.

The two-kbar quenched crystals also showed incipient well-formed crystal faces. However, because of the much slower quench rates in the cold-seal apparatus, it is possible that there was some quench reprecipitation of dissolved silica on the crystals, which would result in underestimation of the solubility. Our measured silica molality in pure H_2O is 0.139 at 700°C, compared to the Anderson and Burnham (1965) value of 0.158 molal at the same conditions (average of two runs).

3.2. Pressure Effect on Solubility and Salting-In

Figure 1 shows the solubility data at 700°C and 1–15 kbar. The drastic change in solubility behavior between 2 and 10–15 kbar is apparent. At 2 kbar there is a strong solubility enhancement effect, with quartz solubility rising steeply with NaCl concentration to a value about 50% higher at $X(H_2O) = 0.9$ than in pure H_2O. The initial rate of salting-in is about the same as at 1 kbar, if a small extrapolation of the data of Xie and Walther (1993) is made of their measurements at m(NaCl) = 0.49 and 0.83 (Fig. 1). The Novgorodov (1977) measurements show the same initial salting-in effect. The apparent crossing of his highest-salinity point at 1.5 kbar above our 2 kbar data could be an artifact of different experimental techniques, though an actual cross-over could conceivably occur in the

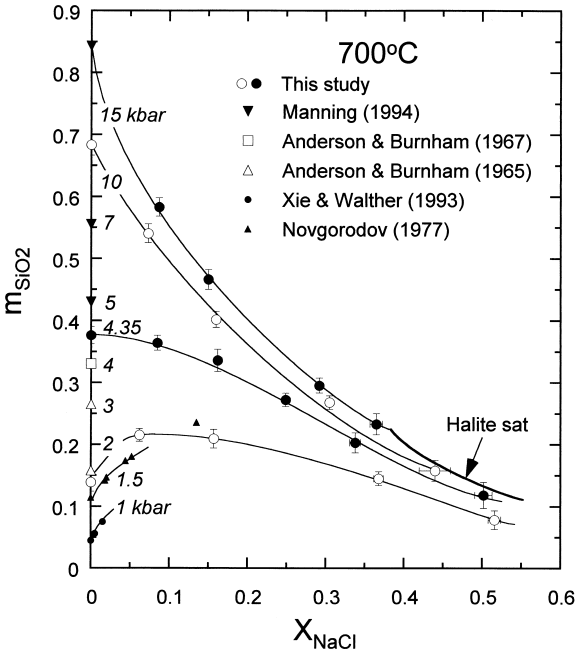

Fig. 1. Comparison of measurements of quartz solubilty in NaCl solutions at 700°C, 1–15 kbar, expressed as molality, $m(SiO_2)$, versus mole fraction of NaCl (X_{NaCl}). The Xie and Walther (1993) points at 1 kbar were extrapolated from the data in their Fig. 2b. Solubility isobars are fit by eye. The position of halite saturation is uncertain because this condition was investigated only at 10 kbar at 700°C. Uncertainties that are smaller than symbol size are not plotted.

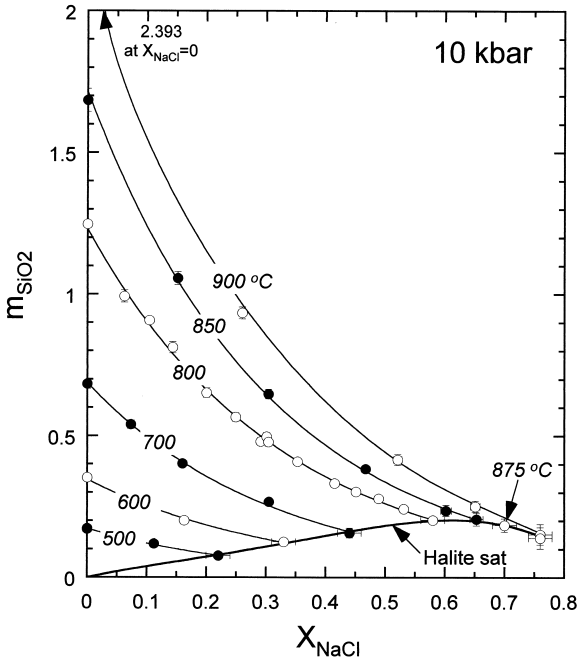

Fig. 2. Quartz solubility measurements at 10 kbar and 500–900°C. Data point of Manning (1994) at 900°C is off-scale. Except at 850°C, all data on the halite-saturation curve represent experiments in which a large halite crystal was present in the quenched charge. X_{NaCl} in these halite-saturated experiments is from Aranovich and Newton (1996). Solubility isotherms are exponential fits to data at $X_{NaCl} < 0.6$ (see text and Fig. 3).

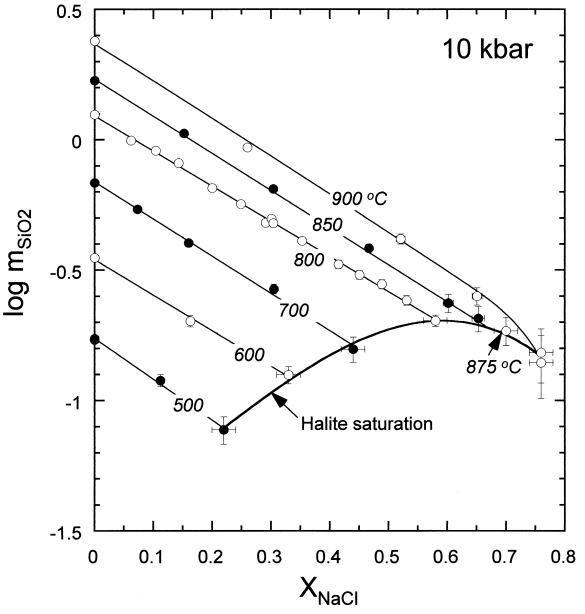

Fig. 3. Data of Fig. 2 on log m(SiO_2) scale, demonstrating exponential dependence of m(SiO_2) on H_2O mole fraction, and that dlog m(SiO_2)/dX_{NaCl} is nearly independent of temperature. This relationship may break down at 900°C and $X_{NaCl} > 0.6$, possibly because of destabilization of hydrous solute silica species at very low H_2O activity.

low-pressure region. At higher salinities, salting-out takes over, but the SiO_2 molality at $X(H_2O) = 0.6$ is still about the same as in pure H_2O. With further increase in salinity, approaching halite saturation, m(SiO_2) is about half of the pure water value. Though the solubility values may be slightly affected by the slow quench in the cold-seal apparatus, the initial salting-in and solubility maximum are undoubtedly real. At 10 and 15 kbar there is only an exponential decrease of solubility with NaCl content of the fluid. At 4.35 kbar, the behavior is intermediate between these extremes, with an initially flat positive d m(SiO_2)/*d* $X(H_2O)$ trajectory, turning with higher salinity into an exponential decline similar to the 10 kbar behavior. The quartz solubility enhancement effect found by Novgorodov (1977) and Xie and Walther (1993) is thus confined to low pressures and low NaCl concentrations. The large spread of solubility in pure H_2O over 2–15 kbar converges to a narrow span in the high NaCl concentration range, ending in halite saturation.

3.3. Exponential Salinity Dependence at High Pressure

At 10 and 15 kbar the solubility shows simple monotonic decrease with NaCl mole fraction at the temperatures investigated. Figure 2 shows the 10 kbar data. The decrease is exponential except possibly at the highest T and X(NaCl) studied. This behavior is clearly shown in the plot of Figure 3 of log m(SiO_2) versus $X(H_2O)$ at 10 kbar. The linearity is striking, especially in the near parallelism of the slopes at all temperatures. This regularity of the solubility implies that, at pressures approaching 10 kbar, a relatively simple medium for SiO_2 solution exists, while at lower pressures, the solvent is more complex, with composition- and pressure-dependent mixtures of solute species. Departure from the linear log m(SiO_2) versus $X(H_2O)$ trend may be present in the highest-salinity point at 900°C and 10 kbar, where salinity can exceed 50 mole percent NaCl before halite saturation occurs. The halite-saturation boundary bends accordingly as silica solubilities begin to drop at $X(H_2O) < 0.5$. The indication that SiO_2 solubilities become markedly lower at very low H_2O activities implies that the dominant solute silica species is a hydrate. The nature of the limiting slopes in Figures 2 and 3 at very high salinities is uncertain: if SiO_2 is insoluble in pure molten NaCl, the slope is undefined.

3.4. Temperature Independence of Relative Molality at High Pressure

The pressure-induced change in SiO_2 solution is shown even more dramatically in Figure 4. In the plot of m(SiO_2)/m_o(SiO_2) at 10 kbar, where m_o refers to quartz solubility in pure H_2O, the data at all temperatures describe a single exponential decline with X(NaCl). The curve through the points is an exponential fit to all 10 kbar data. No systematic temperature dependence of m/m_o is evident. The data at 15 kbar fall nearly on the 10 kbar trend, and are not shown. The corresponding curve for 4.35 kbar is more complex. The experimental data for this pressure in the range 600–750°C describe a trend, though some temperature dispersion seems to be present. At 2 kbar and 700°C, the trend is grossly different because of the salting-in effect.

The observation that relative silica concentration is independent of temperature at high pressures provides a basis for a

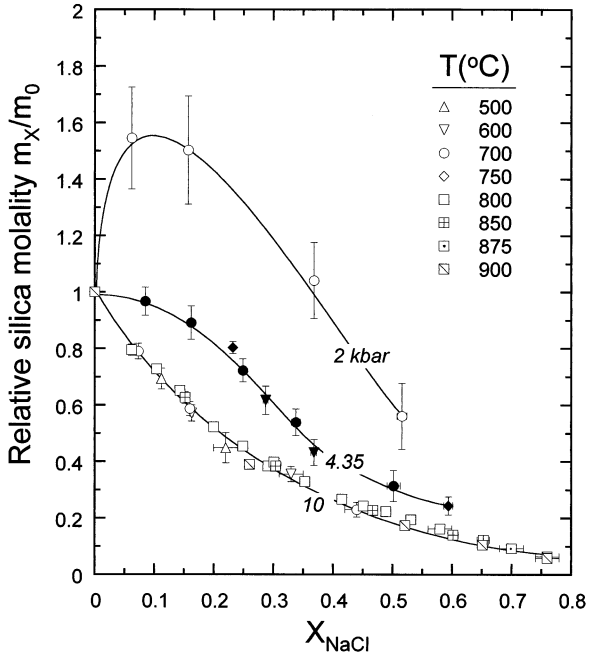

Fig. 4. SiO_2 solubility relative to that in pure H_2O at the same P,T conditions, $m_x(SiO_2)/m_o(SiO_2)$. The plot shows the extreme effect of pressure on silica solubility, in that salting-in (NaCl enhancement of solubility) occurs at 2 kbar, whereas exponential salting out is observed at 10 kbar. Behavior is intermediate at 4.35 kbar.

single expression for estimating quartz solubility in H_2O-NaCl fluids at high pressures and temperatures. We fit polynomials to the 4.35, 10, and 15 kbar data and then used interpolation to estimate the variation in relative molality with pressure at constant temperature. This led to the following equation:

$$\frac{m_{SiO_2}}{m_{0,SiO_2}} = \sum_{j=0}^{3}\sum_{i=0}^{4} \nu_{ij} X_i P_j \qquad (3)$$

The parameters ν_{ij} are given in Table 3 and the predicted variation of $m(SiO_2)/m_o(SiO_2)$ is given in Figure 5A. Figure 5B illustrates the differences between relative molality predicted by Eqn. (3) and determined experimentally. The differences average less than 0.1%, with one standard deviation of 5.3% when all experiments at ≥4.35 kbar are considered. Deviations are slightly skewed towards positive values. The standard deviation decreases to 4.9% when X(NaCl) ≤ 0.5 is considered, and to 3.9% when using only the 10 and 15 kbar data. Thus, Eqn. (3) is expected to provide an accurate value to within

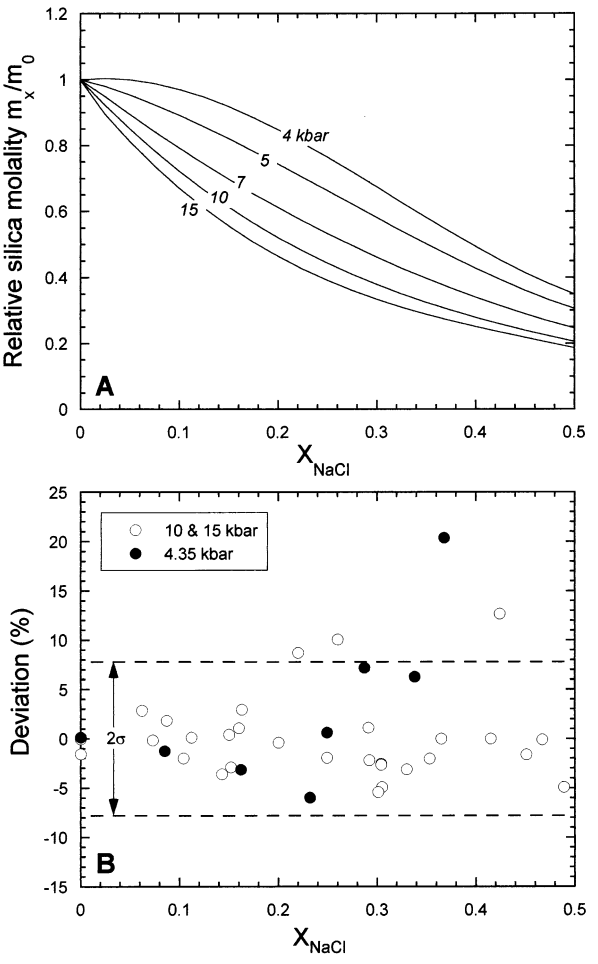

Fig. 5. (A) Temperature-independent isobars of relative quartz solubility from Eqn. (3), text. (B) Difference, in percent, between relative silica molality predicted by Eqn. (3), text, and experimental determinations at the same temperatures and pressures. The low-pressure data (4.35 kbar) display increasing deviation from the equation with increasing X_{NaCl}. Although devations for the high-pressure (10–15 kbar) data are greatest at high X_{NaCl}, there is no systematic trend with fluid composition. The region between the dashed lines corresponds to two standard deviations in the difference for 10–15 kbar data.

about 10% at the 2σ level at 500–900°C, 4–15 kb, and $0 < X(NaCl) \leq 0.5$. It is not valid outside this range. Table 4 lists values of $m(SiO_2)/m_o(SiO_2)$ calculated with Eqn. (3) at discrete pressure and X(NaCl) values.

Our analysis predicts that silica solubility at 4 kbar is nearly independent of salinity to X(NaCl) = 0.15 (Fig. 5A). A very

Table 3. Parameters for equation 1.

		i =				
		0	1	2	3	4
	0	0.96907	0.012348	−0.00129	3.65E-05	−7.31E-08
	1	10.418	−4.0242	0.46876	−0.02565	0.000539
j =	2	−41.383	13.996	−1.689	0.095512	−0.00206
	3	38.761	−12.961	1.6059	−0.09275	0.002024

Table 4. Relative molality (m_i/m_o) from equation 1.

P (kbar)	X(NaCl) 0.05	0.10	0.15	0.20	0.25	0.30	0.35	0.40	0.45	0.50
4	1.000	0.971	0.918	0.848	0.765	0.674	0.582	0.494	0.414	0.349
5	0.954	0.892	0.821	0.744	0.663	0.581	0.502	0.428	0.361	0.305
6	0.920	0.834	0.750	0.667	0.588	0.512	0.442	0.377	0.320	0.271
7	0.895	0.792	0.698	0.612	0.533	0.461	0.397	0.340	0.289	0.246
8	0.876	0.762	0.661	0.572	0.493	0.425	0.365	0.312	0.267	0.227
9	0.862	0.740	0.634	0.543	0.465	0.398	0.341	0.293	0.251	0.214
10	0.850	0.722	0.613	0.521	0.443	0.379	0.324	0.279	0.240	0.205
11	0.840	0.708	0.596	0.504	0.427	0.364	0.312	0.269	0.232	0.199
12	0.831	0.695	0.582	0.489	0.414	0.352	0.303	0.262	0.227	0.195
13	0.823	0.684	0.570	0.478	0.403	0.344	0.296	0.257	0.223	0.191
14	0.817	0.676	0.561	0.469	0.395	0.337	0.291	0.253	0.220	0.188
15	0.813	0.671	0.556	0.464	0.391	0.334	0.288	0.251	0.218	0.186

small absolute salting-in may occur at low salinity at that pressure. Figure 5A shows that the salting-in tendency inherited from low pressures is expected to result in elevated relative solubility to no more than about 5–6 kbar, above which there is a nearly exponential decrease in solubility with increasing X(NaCl). The loss of the salting-in effect with increasing pressure can also be visualized in a three-dimensional perspective view (Fig. 6).

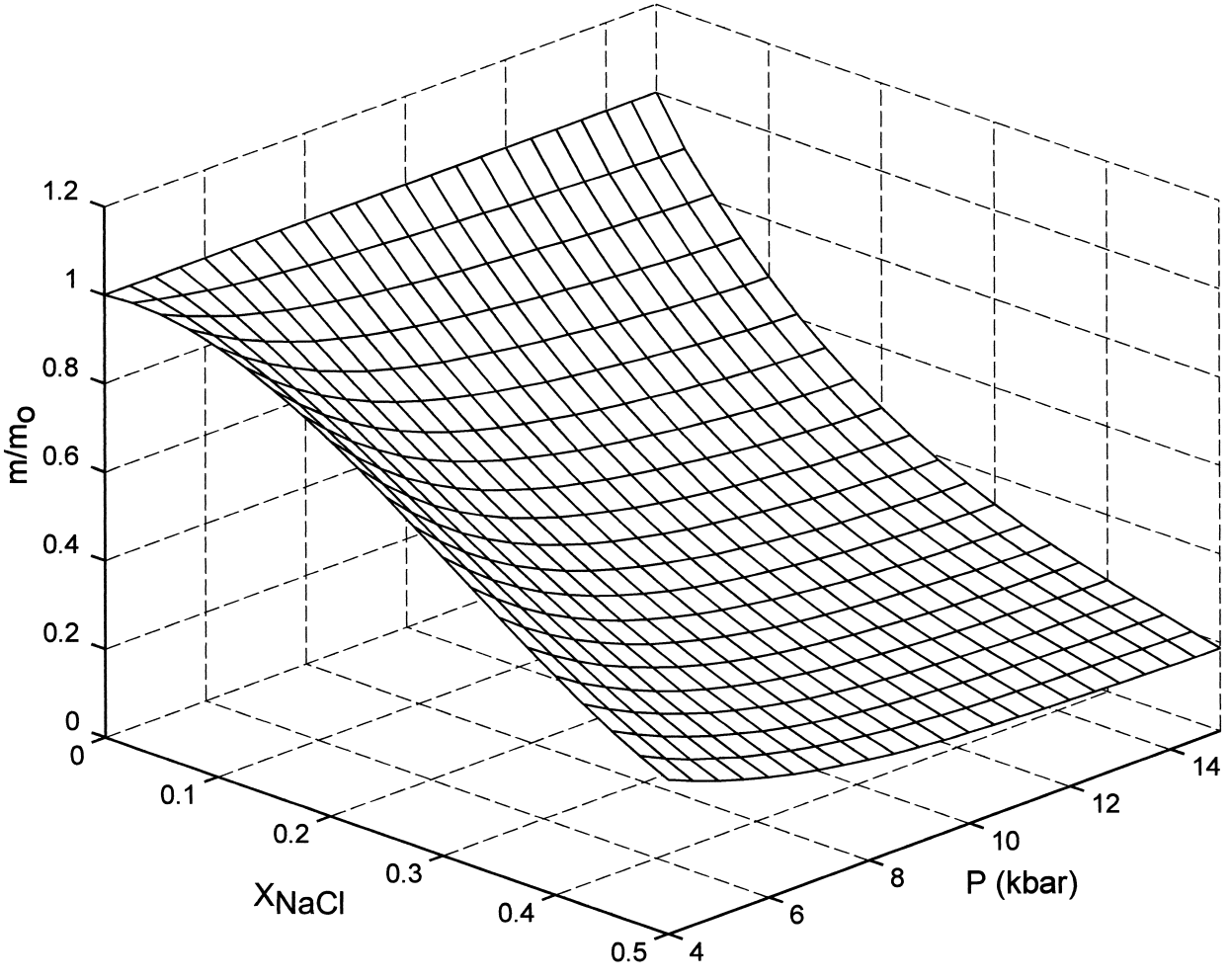

Fig. 6. Perspective view of the temperature-independent relative quartz solubility surface as a function of X_{NaCl} and pressure.

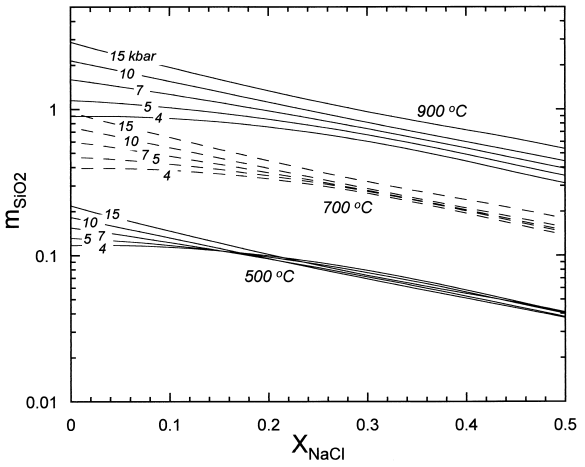

Fig. 7. Silica molality as a function of NaCl mole fraction as predicted by Eqn. (3), text, at 500, 700, and 900°C and 4–15 kbar. The great regularity of solute behavior at $X_{NaCl} > 0.2$ indicates that the fluids attain a simple constitution at high pressure and NaCl concentrations, which may be viewed as an ionic hydrosaline magma.

Figure 7 shows silica concentrations in H_2O-NaCl fluids in equilibrium with quartz at 500, 700, and 900°C, 4–15 kbar, and X(NaCl) = 0–0.5 and Figure 8 shows SiO_2 molality isopleths at 500–900°C at 100°C intervals. Equation (3) was used in combination with predicted values of $m_o(SiO_2)$ from Manning (1994) to generate these figures. Figures 7 and 8 illustrate that at 500–600°C, X(NaCl) > 0.2, there is very little difference in silica concentration over the entire pressure range at fixed X(NaCl). Thus, in general, pressure does not strongly influence quartz solubility in concentrated brines at low temperatures and P > 4 kb. At higher temperatures, the isopleths display progressively greater separation because $m_o(SiO_2)$ increases with P and T (Fig. 8C–E).

3.5. Solubility in CO_2-H_2O Solutions

Quartz solubility measurements in CO_2-H_2O solutions at 10 kbar and 800°C (Table 2) are subject to larger uncertainties than the NaCl-H_2O data at the same conditions because of the small solubilities, as well as the requirement of smaller crystals and fluid volumes. Trial extrapolation of the lower-pressure data of Shettel (1974) shows that, unlike in NaCl solutions at low pressues, solubility in the CO_2-H_2O system is fairly regular and predictable with changing T and P. The following equation, derived in part from the lower P,T data as summarized by Walther and Orville (1983), reproduces the present measurements in CO_2-H_2O solutions at 10 kbar and 800°C within uncertainties:

$$m(SiO_2) = 0.0301\{\exp[3.76 \times (H_2O)] - 1\} \quad (4)$$

Figure 9 shows $m(SiO_2)$ versus H_2O activity, $a(H_2O)$. The standard state of H_2O is the pure phase at any temperature and pressure. Activities are consistent with Aranovich and Newton (1996) for NaCl solutions and Aranovich and Newton (1999) for CO_2 solutions. The large difference in silica solubility behavior between the two media occurs because of the opposite mixing properties of the CO_2-H_2O and NaCl-H_2O systems at elevated pressures: in NaCl solutions the H_2O activities are much lower than the mole fractions at pressures above 4 kbar, by virtue of pressure-induced ionic dissociation (Aranovich and Newton, 1996), whereas increasing pressure causes H_2O activities to exceed the mole fractions in CO_2 solutions by substantial amounts above 5 kbar. Figure 9 shows that quartz is as much as an order of magnitude more soluble in concentrated NaCl solutions than in CO_2 solutions of the same H_2O activity, in the low $a(H_2O)$ range (<0.5).

4. DISCUSSION AND INTERPRETATION

A principal finding of the present investigation is the change with pressure from initial enhancement of SiO_2 solubility in NaCl solutions at 2 kbar to initial salting-out at pressures above ~4 kbar, as shown in Figures 1 and 4. This behavior closely parallels the large decrease of H_2O activity with increasing pressure, produced undoubtedly by dissociation of a neutral solute $NaCl^o$ complex into Na^+ and Cl^- ions as H_2O densities increase above about 0.7 gm/cm^3 (Aranovich and Newton, 1996). It seems highly probable, therefore, that the change from salting-in to salting-out is occasioned by dissociation of $NaCl^o$ into ions. Indeed, two different solution regimes appear to exist, with contrasting effects on silica solubility. At low solution densities, encountered at low pressure and low salinity, the salting-in of SiO_2 is maximized. At high solution densities, change in silica solubility with increasing salinity is more regular, with monotonic salting-out. This fundamental change in solution behavior may be characterized as the transition from complex high-temperature aqueous solutions dominated by the neutral $NaCl^o$ complex, to ionic solutions, or hydrosaline melts, exhibiting remarkably regular SiO_2 solubility behavior over large ranges of T, P, and salinity, as illustrated in Figures 3 and 7.

It is easily shown that the exponential decrease of quartz solubility with increasing NaCl concentration at 10 kbar is an expected effect if the solubility is very low in molten NaCl, and if the solution is a simple mixture of ions and molecules without excess enthalpy or non-configurational entropy. A significant change of slope of the plot of log SiO_2 molality versus H_2O mole fraction (Fig. 3), may exist in the 900°C isotherm below $X(H_2O) = 0.5$, possibly signalling a change in constitution of the solute silica species. An accelerated decrease in solubility at high salinity would imply that the dominant silica solute species is a hydrate, which is expected to become unstable at very low H_2O activities.

The nature of the silica solute species may be investigated in the plot of log $m(SiO_2)$ versus log H_2O activity, following Walther and Orville (1983), as shown in Figure 10. The slope of the trend in H_2O-NaCl solutions suggests that the dominant solute species is H_4SiO_4, with possible admixture of a silica monohydrate at lower H_2O activities. The change to lower hydration state would be consonant with decreasing H_2O activity, which must progressively destabilize hydrous solute species. This analysis assumes that there is no significant Na-bearing solute complex, such as that suggested by Anderson and Burnham (1983). Our data do not rule out the latter possibility.

A similar analysis for the present solubility data in CO_2-H_2O solutions (Fig. 10) indicates that the dominant dissolved silica

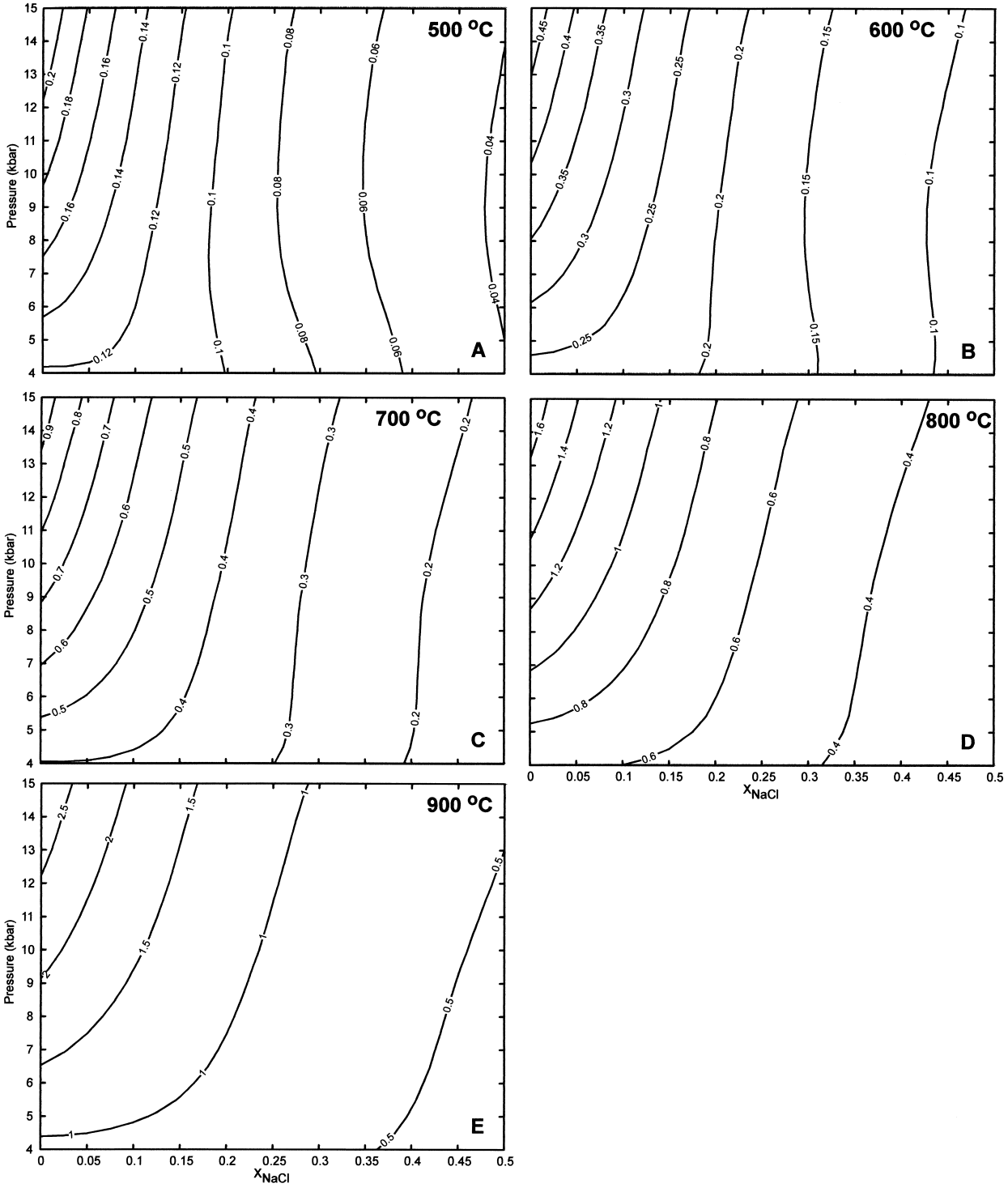

Fig. 8. (A–E). Silica molality isopleths at 500–900°C as a function of pressure and X_{NaCl} as determined by Eqn. (3), text.

species is a neutral dihydrate with one to three attached (solvated) H_2O molecules, the solvation number decreasing with decreasing H_2O activity. This is virtually the same behavior as found by Walther and Orville (1983) at pressures of 5 kbar and below. It is apparent that the aqueous solubility behavior of quartz is much different in NaCl-bearing than in CO_2-bearing solutions.

The two disparate theories of SiO_2 solubility in NaCl solutions may be contrasted, especially with regard to the origin of the salting-in effect. Xie and Walther (1993), after a detailed

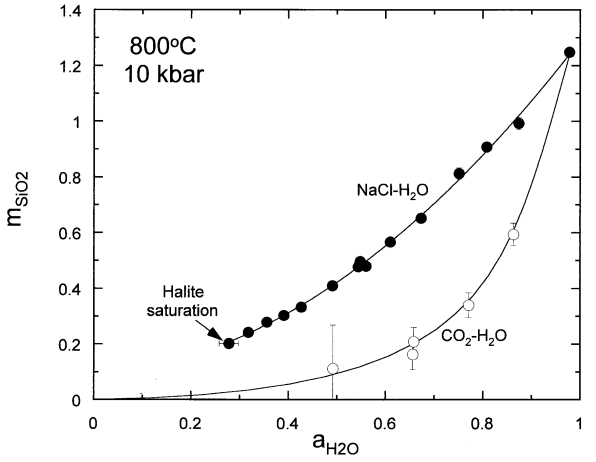

Fig. 9. Comparison of silica solubility at 10 kbar and 800°C in concentrated NaCl-H_2O and CO_2-H_2O solutions as functions of H_2O activity (a_{H_2O}). The plot shows that dissolved SiO_2 partitions preferentially into concentrated salt solutions relative to CO_2-rich fluids. Because such fluids are immiscible over a wide range of high P-T, the data illustrate that silica will be strongly fractionated into the brine. The large error bars at low H_2O activity result from the low solubility of quartz in CO_2-rich fluids. H_2O activities in NaCl solutions from Aranovich and Newton (1996) and in CO_2 solutions from Aranovich and Newton (1999).

analysis of the electrostatics of NaCl-H_2O solutions, concluded that the neutral $NaCl^o$ complex does not have sufficient dipole moment to account for the magnitude of the observed salting-in effect at 0.5 to 2 kbar. They appealed instead to both solvation and short-range electrostatic interactions between dissociated

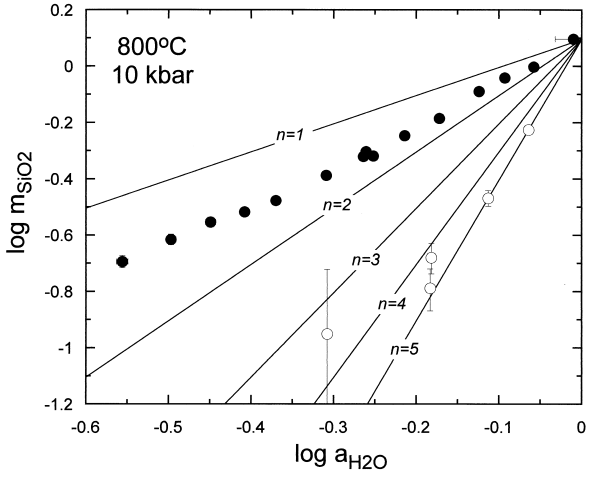

Fig. 10. Log m(SiO_2) versus log a(H_2O) at 800°C and 10 kbar. Present experimental data for CO_2-H_2O solutions lie in the sector between slopes of n = 3 and n = 5. Following Walther and Orville (1983), n is interpreted as the total hydration number of the dominant solute silica species, necessarily decreasing with increasing salinity. If the same interpretation is applicable to the data for NaCl solutions, the hydration number would decrease with decreasing H_2O activity from 1.9 in pure H_2O to 1.1 at a(H_2O) = 0.3. The plot shows that an entirely different solution mode exists for quartz in concentrated electrolyte solutions at high pressures than for solutions in a solvent containing a neutral non-polar component.

Na^+ and Cl^- ions and H_2O molecules, with resultant increase of the dielectric constant of the solution. In this approach, variations in silica molality with X(NaCl) are related through the Setchenow equation:

$$\log \gamma(SiO_2) = b' I \quad (5)$$

In this equation, I is the ionic strength of the solution, defined as one-half the sum of the molalities of charged species, b′ is the empirical Setchenow coefficient, which is a function of T and P, and adopting a standard state for aqueous SiO_2 of unit activity of the hypothetical one molal solution at infinite dilution at a given pressure and temperature, $\gamma(SiO_2)$ is the ratio of SiO_2 molality in pure H_2O to that in H_2O-NaCl solution. In Eqn. (5), negative values of b′ promote small values of $\gamma(SiO_2)$ and hence salting-in.

Xie and Walther (1993) fitted Eqn. (5) to their solubility data at 0.5 and 1.0 kbar to explain the observed high-temperature salting-in and low-temperature salting-out. Their reconstruction assumes that no complexing takes place between dissolved silica and solute ions. The approach of Anderson and Burnham (1983) is quite different from that of Xie and Walther (1993) in that the salting-in would be explained by the SiO_2 solution reaction with NaCl, according to Eqn. (2).

Both theories have shortcomings in application to the present study. The Xie and Walther (1993) reconstruction must be regarded as mainly empirical, since the calculated Setchenow coefficients show large variation over relatively small ranges of T and P, and it is uncertain how to extrapolate the low pressure results to mid- and lower-crustal pressures. The solute reaction theory of Anderson and Burnham (1983) predicts that the solutions become quite acid for SiO_2-rich solutions, which is questionable. An attempt by these authors to calculate an equilibrium constant for the reaction assumes that, apart from the salting-in effect produced by reaction (2), NaCl solutions would have the same effect on SiO_2 solubility as CO_2 solutions at the same X(H_2O). Figure 10 shows that, for the conditions of 800°C and 10 kbar, where there is no salting-in, the solution mechanisms are quite different in the two media. Neither theory allows for the close correspondence between salting-out behavior and pressure-induced decrease of H_2O activity.

In a more general way, it seems clear why addition of NaCl at high pressures should decrease the concentration of silica faster than at low pressures. In Eqn. (1), if n = 2, the equilibrium constant is $K(T,P) = a(H_4SiO_4)/a^2(H_2O)$. At ten kbar and high temperature, the H_2O activity is nearly equal to the square of the mole fraction in NaCl solutions (Aranovich and Newton, 1996), whereas at 2 kbar, the activity is close to the mole fraction. Hence, the activity (and concentration) of H_4SiO_4 will fall faster at 10 kbar with increasing salinity than at 2 kbar, with consequently greater tendency to overcome any salting-in effect.

5. APPLICATION TO PETROLOGY

Several mechanisms have been suggested for generation of concentrated alkali-chloride solutions during crustal processes. At shallow depths, a hyperconcentrated brine or hydrosaline melt may result from fluid immiscibility at high temperatures, most plausibly in cooling of fluids of magmatic origin (Fournier, 1987). At deeper levels, pore fluids may be enriched

in solutes by extraction of H_2O into anatectic melts (Philippot, 1993), by preferential absorption of H_2O in hydration reactions (Bennett and Backer, 1992; Markl and Bücher, 1998; Kullerud and Erambert, 1999), by prograde dehydration reactions in deeply subducted serpentinite and sea-floor sediments (Scambelluri et al., 1997), or as magmatic exhalations from crystallizing mafic magmas in deep-crustal environments (Hansteen and Burke, 1994). Although phase relations in the ternary system H_2O-NaCl-CO_2 are still imperfectly known at high temperatures and pressures, it is likely that fluid immiscibility exists between concentrated brines and CO_2-rich fluids at most P-T conditions prevailing in high-grade metamorphism (Duan et al., 1995).

The present work shows that NaCl solutions at deep-crustal metamorphic conditions are substantial solvents for silica, despite the strong decrease of quartz solubility with NaCl concentration. At 10 kbar and 800°C, a concentrated brine of H_2O mole fraction 0.6 will have a H_2O activity of 0.45, according to Aranovich and Newton (1996), and, according to the experimental work of Aranovich and Newton (1998), the H_2O activity is low enough to stabilize orthopyroxene in biotite-bearing rocks. This solution would dissolve about 0.7 wt.% of SiO_2 in quartz-bearing rocks, according to the present solubility study, or about the same as in pure water at 1 kbar and 800°C. Such fluids could account for the synmetamorphic orthopyroxene-bearing quartz veins found in some classic granulite facies terranes (e.g., Bamble, S. Norway—Van den Kerkhof et al., 1994; S. India—Hansen et al., 1995). The alternative low-H_2O-activity fluid which has been often cited for granulite facies metamorphism, namely CO_2-rich fluids, would be much more inert, with a silica solubility eight times lower at the same H_2O activity. The vapor-absent interpretation of granulite facies metamorphism (Lamb and Valley, 1984) could not account for the quartz-orthopyroxene veins. The additional properties of high alkali mobility and grain wetting ability, again in contrast to CO_2-rich fluids, make concentrated alkali chloride solutions seem feasible as chemically active agents in deep-crustal metamorphism.

An alkali-rich, low-H_2O activity fluid provides a conceptual model for interpretation of many features of metamorphic rocks, including migmatites, albitization, myrmekite, and replacement antiperthite (Newton et al., 1998). The ability of hypersaline fluids to exchange alkalis in deep-seated environments without large-scale rock melting is enhanced by their extraordinary ability to infiltrate low-porosity silicate aggregates along grain boundaries. Metasomatic effects could be quite substantial, even for small fluid-rock ratios, because of the very high alkali contents of concentrated brines. The solubility of silica as feldspar-like molecules may be considerably higher than in the simple system SiO_2-H_2O-NaCl, and higher silica solubility is expected in alkaline solutions, such as those involved in fenitization. Silica solubility in more complex systems is an important area for further investigation.

The uniformity of silica solubility in concentrated NaCl solutions at 4 to 15 kbar is noteworthy. At 700°C, solutions of $X(H_2O) = 0.6$ have a very small range of silica solubility at these pressures, less than 20 percent variation. The regularity of silica solubility in high-pressure brines is illustrated in Figures 3 and 7. Apparently, completely ionized brines are relatively simple substances, which become more complex in their behavior at lower pressures and fluid densities as the $NaCl^o$ neutral complex becomes stable. In this regard, a completely ionized NaCl solution may be a more convenient standard state for solute silica than the traditional dilute solution state at low pressure, which, as this study shows is not suitable for prediction of quartz solubility in brines over most of the pressure-temperature-concentration ranges of deep crust/upper mantle metamorphism.

Acknowledgments—Primary funding for this project was from a National Science Foundation grant for the study of mineral-fluid interactions, EAR-9405999. Mostafa Fayek and Marty Grove generously assisted with the experiments in cold-seal apparatus. John Walther provided helpful discussions of our preliminary results, and he and Bob Bodnar critically reviewed the manuscript. Tom LaTourrette alerted us to pertinent recent literature.

REFERENCES

Ague J. J. (1994) Mass transfer during Barrovian metamorphism of pelites, south-central Connecticut. I.: Evidence for changes in composition and volume. *Am. J. Sci.* **294,** 989–1057.

Anderson G. M. and Burnham C. W. (1965) The solubility of quartz in supercritical water. *Am. J. Sci.* **263,** 494–511.

Anderson G. M. and Burnham C. W. (1967) Reaction of quartz and corundum with aqueous chloride and hydroxide solutions at high temperatures and pressures. *Am. J. Sci.* **285,** 12–27.

Anderson G. M. and Burnham C. W. (1983) Feldspar solubility and the transport of aluminum under metamorphic conditions. *Am. J. Sci.* **283–A,** 283–297.

Aranovich L. Y. and Newton R. C. (1996) H_2O activity in concentrated NaCl solutions at high pressures and temperatures measured by the brucite-periclase equilibrium. *Contrib. Mineral. Petrol.* **125,** 200–212.

Aranovich L. Y. and Newton R. C. (1997) H_2O activity in concentrated KCl and KCl-NaCl solutions at high temperatures and pressures measured by the brucite-periclase equilibrium. *Contrib. Mineral. Petrol.* **127,** 261–271.

Aranovich L. Y. and Newton R. C. (1998) Reversed determination of the reaction: Phlogopite + quartz = enstatite + potassium feldspar + H_2O in the range 750–875°C and 2–12 kbar at low H_2O activity with concentrated KCl solutions. *Am. Mineral.* **83,** 193–204.

Aranovich L. Y. and Newton R. C. (1999) Experimental determination of CO_2-H_2O activity-composition relations at 600–1000°C and 6–14 kbar by reversed decarbonation and dehydration reactions. *Am. Mineral.* **84,** 1319–1332.

Belkin H. E., DeVivo B., Lima A., and Torok K. (1997) Magmatic (silicates/saline/sulfur-rich/CO_2) immiscibility and zirconium and rare-earth enrichment from alkaline magma chamber margins, evidence from Ponza island, Pontine archipelago, Italy. *Eur. J. Mineral.* **8,** 1401–1420.

Bennett D. G. and Barker A. J. (1992) High salinity fluids: The result of retrograde metamorphism in thrust zones. *Geochim. Cosmochim. Acta* **56,** 81–95.

Chen C.-T. A. and Marshall W. L. (1982) Amorphous silica solubility: IV. Behavior in pure water and aqueous sodium chloride, sodium sulfate, magnesium chloride, and magnesium sulfate solutions up to 350°C. *Geochim. Cosmochim. Acta* **46,** 279–287.

Crawford M. L. and Hollister L. S. (1986) Metamorphic fluids, the evidence from fluid inclusions. In *Fluid-rock Interactions During Metamorphism* (eds. J. V. Walther and B. J. Wood) Springer, Berlin. pp. 1–35.

Duan Z., Møller N., and Weare J. H. (1995) Equation of state for NaCl-H_2O-CO_2 system. Prediction of phase equilibria and volumetric properties. *Geochim. Cosmochim. Acta* **59,** 2869–2882.

Fournier R. O., Rosenbauer R. J., and Bischoff J. L. (1982) The solubility of quartz in aqueous sodium chloride solutions at 350°C and 180 to 500 bars. *Geochim. Cosmochim. Acta* **46,** 1969–1978.

Fournier R. O. (1987) Conceptual models of brine evolution in magmatic-hydrothermal systems. *U.S. Geol. Surv. Prof. Paper* **1350,** 1487–1506.

Gibert F., Guillaume D., and LaPorte D. (1998) Importance of fluid immiscibility in the H_2O-NaCl-CO_2 system and selective CO_2 entrapment in granulites: Experimental phase diagram at 5–7 kbar, 900°C and wetting textures. *Eur. J. Mineral.* **10,** 1109–1123.

Hansen E. C., Newton R. C., Janardhan A. S., and Lindenberg S. (1995) Differentiation of Late Archean crust in the Eastern Dharwar Craton, Krishnagiri-Salem area, South India. *J. Geol.* **103,** 629–651.

Hansteen T. H. and Burke E. A. J. (1994) Melt-mineral-fluid interaction in the Oslo Rift, southeast Norway: II. High-temperature fluid inclusions in the Eikern-Skrim complex. *Contrib. Mineral. Petrol.* **107,** 242–254.

Johannes W. (1973) A simplified piston-cylinder apparatus of high precision. *N. Jahrb. Mineral.* **H7/8,** 331–351.

Kennedy G. C. (1950) A portion of the system silica-water. *Econ. Geol.* **45,** 629–653.

Koster Van Groos A. F. (1991) Differential thermal analysis of the liquidus relations in the system NaCl-H_2O to 6 kbar. *Geochim. Cosmochim. Acta* **55,** 2811–2817.

Kullerud K. and Erambert M. (1999) Cl-scapolite, Cl-amphibole, and plagioclase equilibria in ductile shear zones at Nusfjord, Lofoten, Norway: Implications for fluid compositional evolution during fluid-mineral interaction in the deep crust. *Geochim. Cosmochim. Acta* **63,** 3829–3844.

Lamb W. and Valley J. W. (1984) Metamorphism of reduced granulites in low CO_2 vapour-free environment. *Nature* **312,** 56–58.

Lowell R. P., Van Cappellen P., and Germanovich L. N. (1993) Silica precipitation in fractures and the evolution of permeability in hydrothermal upflow zones. *Science* **260,** 192–194.

Lowenstern J. B. (1994) Chlorine, fluid immiscibility, and degassing in peralkaline magmas from Pantelleria, Italy. *Am. Mineral.* **79,** 353–369.

Manning C. E. (1994) The solubility of quartz in the lower crust and upper mantle. *Geochim. Cosmochim. Acta* **58,** 4831–4839.

Manning C. E. (1995) Phase-equilibrium controls on SiO_2 metasomatism by aqueous fluids in subduction zones: Reaction at constant pressure and temperature. *Int. Geol. Rev.* **37,** 1074–1093.

Manning C. E. (1997) Coupled reaction and flow in subduction zones: Silica metasomatism in the mantle wedge. In *Fluid Flow and Transport in Rocks* (eds. B. Jamtveit and B. W. D. Yardley) pp. 139–148. Chapman & Hall.

Markl G. and Bücher K. (1998) Composition of fluids in the lower crust inferred from metamorphic salt in lower crustal rocks. *Nature* **391,** 781–783.

Mirwald P. W., Getting I. C., and Kennedy G. C. (1975) Low-friction cell for piston-cylinder high-pressure apparatus. *J. Geophys. Res.* **80,** 1519–1525.

Morey G. W. and Hesselgesser J. M. (1951) The solubility of some minerals in supercritical steam at high pressures. *Econ. Geol.* **46,** 821–835.

Newton R. C., Aranovich L. Y., Hansen E. C., and Vandenheuvel B. A. (1998) Hypersaline fluids in Precambrian deep-crustal metamorphism. *Precam. Res.* **91,** 41–63.

Novgorodov P. G. (1977) On the solubiilty of quartz in H_2O + CO_2 and H_2O + NaCl at 700°C and 1.5 kb pressure. *Geochem. International* **14(4),** 191–193.

Philippot P., (1993) Fluid-melt-rock interaction in mafic eclogites and coesite-bearing metasediments: Constraints on volatile recycling during subduction. *Chem. Geol.* **108,** 93–112.

Philippot P. and Selverstone J. (1991) Trace-element-rich brines in eclogitic veins: Implications for fluid composition and transport during subduction. *Contrib. Mineral. Petrol.* **106,** 417–430.

Philippot P., Chevallier P., Chopin C., and Dubessy J. (1995) Fluid composition and evolution in coesite-bearing rocks (Dora Maira massif, western Alps): Implications for element recycling during subduction. *Contrib. Mineral. Petrol.* **121,** 29–41.

Roedder E. (1971) Fluid inclusion studies on porphyry-type ore deposits at Bingham, Utah, Butte, Montana, and Climax, Colorado. *Econ. Geol.* **66,** 98–120.

Saccocia P. J. and Seyfried W. E., Jr (1990) Talc-quartz equilibria and the solubility of magnesium chloride complexes in NaCl-$MgCl_2$ solutions at 300, 350, and 400°C, 500 bars. *Geochim. Cosmochim. Acta* **54,** 3283–3294.

Samson I. M., Liu W., and Williams-Jones A. E. (1995) The nature of orthomagmatic fluids in the Oka carbonatite, Quebec, Canada. *Geochim. Cosmochim. Acta* **59,** 1963–1977.

Scambelluri M., Piccardo G. B., Philippot P., Robbiano A., and Negretti L. (1997) High salinity fluid inclusions formed from recycled seawater in deeply subducted alpine serpentinite. *Earth Planet. Sci. Lett.* **148,** 485–499.

Sciuto, P. F. and Ottonello, G. (1995) Water-rock interaction on Zabargad Island, Red Sea—a case study: I. Application of the concept of local equilibrium. *Geochim. Cosmochim. Acta* **59,** 2187–2206.

Shettel D. L. (1974) The solubility of quartz in supercritical H_2O-CO_2 fluids. M.S. thesis, The Pennsylvania State Univ.

Smit C. A. and Van Reenen D. D. (1997) Deep crustal shear zones, high-grade tectonites, and associated metasomatic alteration in the Limpopo Belt, South Africa. *J. Geol.* **105,** 37–58.

Sorensen S. S. (1988) Petrology of amphibolite-facies mafic and ultramafic rocks from the Catalina Schist, southern California: Metamorphism and migmatization in a subduction zone metamorphic setting. *J. Met. Geol.* **6,** 405–435.

Touret J. L. R. (1985) Fluid regime in southern Norway, the record of fluid inclusions. In *The Deep Proterozoic Crust in the North Atlantic Provinces* (eds. A. C. Tobi and J. L. R. Touret), pp. 517–549. Reidel.

Van den Kerkhof A. M., Touret J. L. R., and Kreulen R. (1994) Juvenile CO_2 in enderbites of Tromøy near Arendal, southern Norway: A fluid inclusion and stable isotope study. *J. Met. Geol.* **12,** 301–310.

Walther J. V. and Orville P. M. (1983) The extraction-quench technique for determination of the thermodynamic properties of solute complexes. Application to quartz solubility in fluid mixtures. *Am. Mineral.* **68,** 731–741.

Watson E. B. and Brenan J. M. (1987) Fluids in the lithosphere: 1. Experimentally-determined wetting characteristics of CO_2-H_2O fluids and their implications for fluid transport, host-rock physical properties, and fluid inclusion formation. *Earth Planet. Sci. Lett.* **85,** 497–515.

Xie Z. and Walther J. V. (1993) Quartz solubilities in NaCl solutions with and without wollastonite at elevated temperatures and pressures. *Geochim. Cosmochim. Acta* **57,** 1947–1955.